Korean J. Chem. Eng., 32(12), 2434-2442 (2015)
DOI: 10.1007/s11814-015-0077-z

pISSN: 0256-1115
eISSN: 1975-7220

Hybrid membranes with low permeability for vanadium redox flow batteries using *in situ* sol-gel process

Su Mi Park and Haekyoung Kim†

School of Materials Science & Engineering, Yeungnam University, 280, Daehak-ro, Gyeongsan, Gyeongbuk 712-749, Korea
(*Received 20 December 2014 • accepted 13 April 2015*)

Abstract−Vanadium redox flow batteries (VRFBs) have been researched as large energy storage systems due to their long cycle life, high energy efficiency, low cost, and flexible design. However, cation exchange membranes are permeable to the vanadium ions in aqueous acidic electrolyte, and vanadium ions crossover reduces the efficiency and capacity of VRFBs. To improve membrane selectivity, proton conducting inorganic materials are proposed for the modification of conventional membranes, e.g., Nafion. Clusters inside Nafion membrane are filled with inorganic materials using *in situ* sol-gel processes, and this results in homogeneous distribution of inorganic materials. Hybrid membranes with Nafion 115 (coded as HN115) exhibit comparable ionic conductivity and a 70% reduced permeability to vanadium ions compared with pristine Nafion 115 (coded as N115). The columbic and energy efficiencies of VRFBs with HN115 at 20 $mA \cdot cm^{-2}$ exhibit higher values of 95% and 80% in their columbic and energy efficiencies, respectively; VRFBs with N115 exhibit 78% and 70%, respectively. The capacity performance is also improved when HN115 is used in VRFBs. The VRFBs with hybrid membranes (lower permeable membrane) show higher columbic efficiency than the VRFB with N115. HN115 exhibit similar columbic efficiency values of 95% over entire current ranges, which are almost unrelated to the current density. However, N115 shows a fluctuating and lower columbic efficiency of 75%, 88%, 93% at 20 $mA \cdot cm^{-2}$, 40 $mA \cdot cm^{-2}$, 80 $mA \cdot cm^{-2}$, respectively. VRFB with N115 (high conductive membrane) exhibits lower voltage drops for discharging and higher energy efficiency at high current ranges. With these results, it is proposed that the energy efficiencies of VRFBs are compromised with membrane conductivity and permeability. The columbic efficiencies are more contributed by membrane permeability. The permeability properties are more dominant in low current density and the ionic conductivity is more effective in high current ranges. To obtain higher performance of VRFBs, the membrane design for selectivity should be considered according to the operation conditions.

Keywords: Hybrid Membrane, Vanadium Redox Flow Battery, Inorganic Proton Conductor, Vanadium Permeability, Efficiencies

INTRODUCTION

Energy conversion technologies that convert renewable energy to electrical energy have been investigated in order to solve problems associated with climate change, and this has resulted in the introduction of more renewable energy technologies, such as wind and solar energy, to the power grid. Energy conversion systems need to store electrical energy for flexible usage. A rechargeable battery could be used as a large energy storage system to store electrical energy; the storage system requires a high charge capacity, low capacity fade, long cycle life, rapid response time, and low cost. Redox flow batteries (RFBs) with various ion combinations have been researched and developed as large-scale energy storage systems. RFBs are rechargeable batteries where two dissolved chemical components in liquid electrolyte separated by a membrane are used to recharge the system. While RFBs have technical advantages over most conventional rechargeable batteries, such as potentially separable liquid tanks and near unlimited longevity, the current attainments are relatively less powerful and require more complicated operation tools. Among the various ion combinations for redox flow batteries (zinc-cerium, zinc-bromine, vanadium-cerium, magnesium-vanadium, vanadium-polyhalide, etc.), vanadium redox flow batteries (VRFBs) have been most researched, developed, and effectively commercialized [1-6]. VRFBs use vanadium ions dissolved in aqueous sulfuric acid, and carbon materials are used as electrode, current collector, and electrolyte supports. Ion exchange membranes are located between the anode and cathode carbon electrodes as separators [7,8]. The advantage of VRFBs over other RFBs is that with using the same metal ions in both electrolytes, the electrodes and membranes are not cross-contaminated and the cell capacity does not decrease over time, which enables a longer life time. However, differences in the metal ion charge oxidations at each electrode exist; therefore, V^{+4}/V^{+5} is used on one side and V^{+2}/V^{+3} is used on the other side, thereby exploiting vanadium to exist in electrolyte in four different oxidation states. V^{+4}/V^{+5} and V^{+2}/V^{+3} should be separated using a membrane to maintain the capacity of vanadium ions. The electrochemical half-reactions of a VRFB are as follows.

$$\text{positive electrode} = VO^{2+} + H_2O \rightleftharpoons VO_2^{+} + 2H^{+} + e^{-}$$
$$\text{negative electrode} = V^{3+} + e^{-} \rightleftharpoons V^{2+}$$

The requirements of VRFBs membranes are high ionic conduc-

†To whom correspondence should be addressed.
E-mail: hkkim@ynu.ac.kr

tivity, low vanadium ion permeability, chemically stable, and low cost. Currently, perfluorinated sulfonic acid polymers, i.e., Nafion, are widely used as membranes in VRFBs due to their good performance and durability. However, Nafion is permeable to vanadium ions and their crossover exhibits ion depletion for redox reactions, which reduces their efficiency and capacity [9]. Toreduce vanadium ion permeability, a significant amount of research has focused on sulfonated aromatic polymer membranes [10-15]. However, sulfonated aromatic polymer membranes exhibit degradation due to backbone oxidation, which cannot tolerate the cyclic environment in VRFBs [16]. Several research groups have also studied anion exchange membranes as potential membranes for VRFBs due to their low cost and low permeability [17-20]. However, the low ionic conductivity and stability of anion exchange membranes in VRFBs exhibits low performance. Perfluorinated membranes (e.g., Nafion), are still good candidates as membranes in VRFBs. Many approaches have been investigated to improve the selectivity of Nafion [21-27]. Composite membranes with inorganic and/or organic materials have been proposed, and they exhibit improved VRFB performance [14,28]. However, the approaches to reduce the permeability induce decreases in the ionic conductivity. With the application of inorganic materials, the ionic conductivity exhibited lowered values for the lowered ion exchange capacity. Furthermore, in order to fabricate composite membranes, the ion exchange polymer solution is mixed with inorganic materials and the membranes are fabricated using a solution casting method, in which it is not easy to obtain homogeneous membranes. The non-uniform dispersion of inorganic particles in polymer membranes causes particle aggregation and can induce defects in the polymer membranes.

In this study, to resolve the conflict between the ionic conductivity and vanadium ion crossover, proton conducting inorganic materials are proposed for the modification of the conventional Nafion membranes, as seen in Fig. 1. *In situ* sol-gel processes are performed inside clusters of Nafion membrane to impregnate the immobilizing inorganic proton conductor, which results in homogeneous distributions of inorganic materials. Hybrid Nafion membranes with inorganic proton conductor fabricated using *in situ* sol-gel process should have improved VRFB performance with lower permeability and comparable ionic conductivity with pristine Nafion membranes.

EXPERIMENTS

1. Membrane Fabrication

Cyclohexane, n-hexanol, dioctyl sulfosuccinate sodium salt, (3-mercaptopropyl) trimethoxysilane ($HS(CH_2)_3Si(OCH_3)_3$), and ammonia (NH_4OH), were purchased from Aldrich® and used without further purification. Nafion membranes were purchased from DuPont and treated with H_2O_2, H_2SO_4 and DI water at 100 °C for 2 h for conversion to H^+ acid forms.

To prepare the hybrid membranes, Nafion 115 and 117 membranes with proton forms were dried at 120 °C for 12 h in a vacuum oven with the process in previous work [29]. The dried membranes were placed in a reaction kettle that was connected to a condenser and water bath of 30 °C. Cyclohexane of 200 g was added to the reaction kettle and stirred with a magnetic stirrer, followed by the addition of 19 g of n-hexanol and 3.1 g of dioctyl sulfosuccinate. After the dioctyl sulfosuccinate was completely dissolved, 4 ml of ammonium hydroxide was added and the reaction mixture was stirred for 30 min. Next, 4.71 g of (3-mercaptopropyl) trimethoxysilane was added and the reaction mixture was stirred for 96 h. After the reaction, the surfaces of the membranes were washed with Kimwipes®, and dried in a vacuum oven at 100 °C for 1 h. The dried membranes were washed with ethanol and dried, followed by washing with acetone and drying at 100 °C in a vacuum oven for 1 h. Finally, the membranes were pretreated with a 1 M H_2SO_4 solution at 100 °C for 2 h, followed by boiling in H_2O at 100 °C for 2 h. The fabricated hybrid membranes were stored in distilled water.

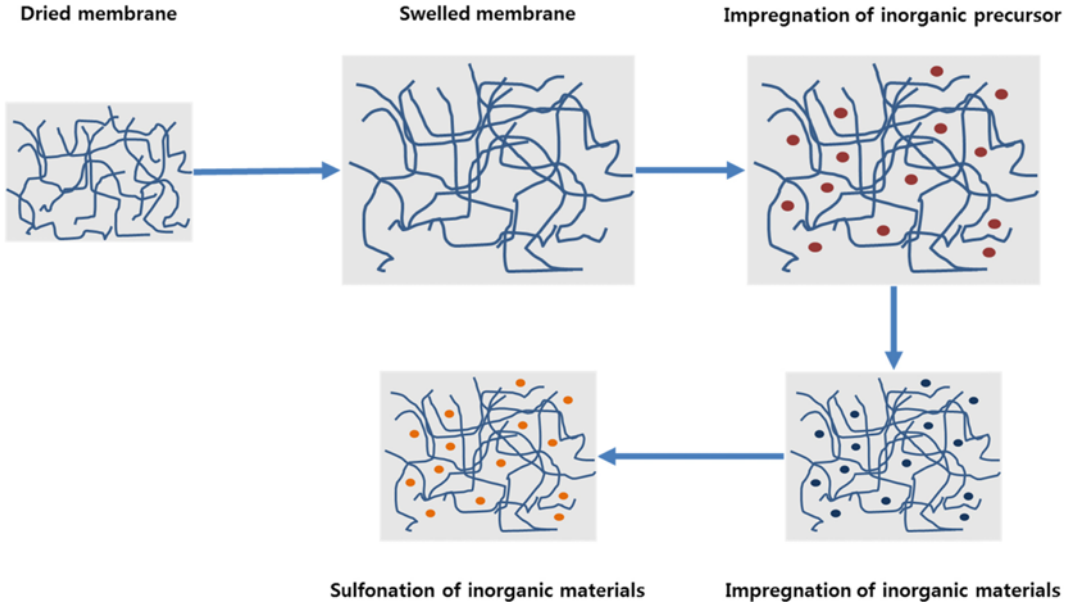

Fig. 1. Schematic diagram of *in situ* sol-gel process for hybrid membrane.

2. Membrane Characterization

Images of the hybrid membranes were characterized using scanning electron microscopy (SEM, FE-SEM 4500, Hitachi, Japan) and energy dispersive X-ray (EDX) analyses. The thermal analyses of the membranes were observed by using thermal gravimetric and the differential thermal analysis measurement (TG-DTA, SDT Q600, TA Instruments, USA).

The hybrid membranes for application as cation exchange membranes in VRFBs were characterized by using their ionic conductivity and VO^{2+} permeability. The ionic conductivity of the membranes was measured with a four-point probe method with an ac impedance analyzer (WEIS®, WONNATECH, Korea) at 100% RH and room temperature. A membrane strip (1.5×1 cm) was fixed in a homemade Teflon cell composed of two outer platinum foils and two inner platinum wires. The resistance (R) of the membrane was measured and the ionic conductivity (σ) was calculated by using σ=L/(A×R), where L and A are the distance between the two inner Pt probes and cross-sectional area of the membrane, respectively, as mentioned at previous work [29].

The vanadium ion crossover of the membranes was measured by using a diffusion cell that consisted of two identical 350 mL volume compartments separated by the membranes. Initially, one compartment was filled with a 2 M H_2SO_4 1 M $MgSO_4$ solution and the other with a 2 M H_2SO_4 1 M $VOSO_4$ solution. It was determined that the absorbance of VO^{+2} increased in 2 M H_2SO_4 1 M $MgSO_4$ solution compartment over time using a UV/VIS spectrometer (GENESYS 10S, ThermoScientific, USA) at room temperature. For comparison, the same measurements were performed with Nafion 115 (N115), hybrid membrane with N115 (HN115), and hybrid membrane with Nafion 117 (HN117). The absorbance of VO^{+2} in hybrid membrane was plotted according to time and compared with that of N115.

3. Measurements of Vanadium Flow Battery Performance

The VRBF performances of the membranes were evaluated by using the flow cell described in Fig. 2. The performance test included a flow cell, two peristaltic pumps, two electrolyte reservoirs and Viton® tubing. Each reservoir included 40 mL of electrolyte, and each electrolyte was circulated at 36 mL/min. Carbon felt (NEWELL, Korea) with a size of 3×3 cm was used as the porous electrode. The felt was used without pre-treatment. The starting electrolyte (1.8 M electrolyte in 3 M H_2SO_4) was used. The anolyte and catholyte were prepared through charging the starting electrolyte to 1.8 V at 40 mA·cm^{-2} using the flow cell. The performance was evaluated through charging to 1.8 V and discharging to 0.8 V at 20, 40 and 80 mA·cm^{-2}. These cycles were repeated 2 to 3 times. The performance of the hybrid membranes (HN115 and HN117) was analyzed and compared with N115 in terms of efficiency and capacity with current density.

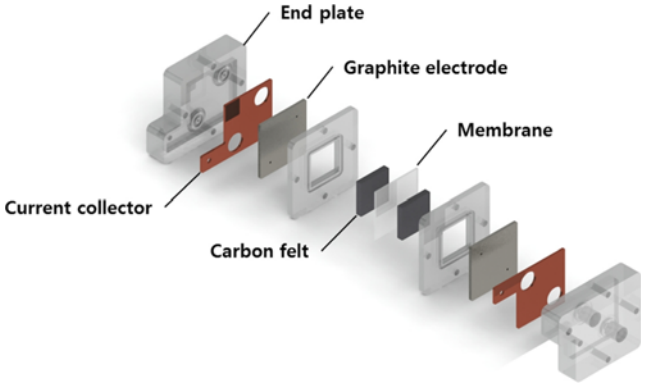

Fig. 2. Schematic diagram of vanadium redox flow battery.

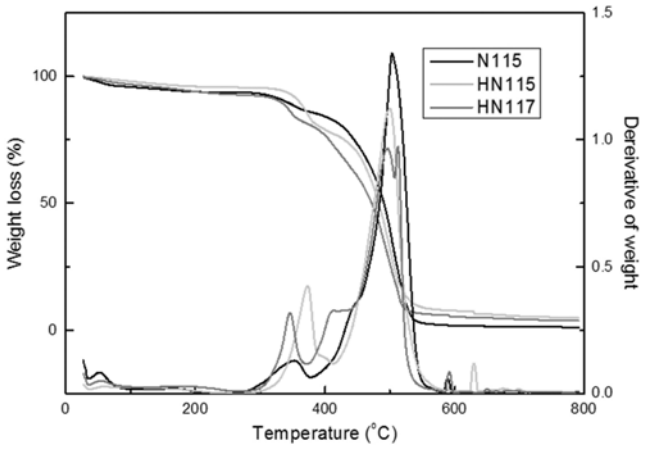

Fig. 3. Thermal analysis curves of membranes.

RESULTS AND DISCUSSION

1. Hybrid Membrane Characterization

As shown in Fig. 3, in the thermal analysis, the first weight losses were observed at 150 °C, which demonstrates that the membranes absorbed water. The water retention performance increased through introducing inorganic materials to the Nafion membrane [30]. Two distinct weight loss steps were observed in the membranes at separate temperature ranges. The impregnation of the inorganic proton conductor affected the material decomposition. The weight losses at 300-400 °C resulted from the separation of the sulfonic acid groups in the N115 and hybrid membranes (HN115 and HN117). The weight losses, which began at approximately 420-520 °C, were attributed to the decomposition of the Nafion main chain. With the inorganic proton conductor in the sulfonic acid group, greater separation of the sulfonic group from the hybrid membranes was observed, which demonstrated the successful impregnation of the proton conductors inside the Nafion. The SEM images and EDX spectrum from the membranes demonstrated that the inorganic proton conductors were impregnated in the Nafion membrane as seen in Fig. 4. The Si element was detected in HN115 and HN117; a higher amount of Si was observed in HN117 than HN115 due to the thicker thickness of Nafion117. The oxygen peaks from the SiO_2 linkage of inorganic proton conductors were also observed in HN115 and HN117.

Fig. 5 presents the ionic conductivity and permeability of N115, HN115 and HN117. Hybrid membranes exhibited comparable ionic conductivity over 0.08 S·cm^{-1} and 70% lowered permeability values: N115 with 0.1 S·cm^{-1}, HN115 with 0.085 S·cm^{-1}, 30% of N115, and HN117 with 0.08 S·cm^{-1}, 28% of N115 (membrane with ionic conductivity, relative permeability vs. N115). Here, the inor-

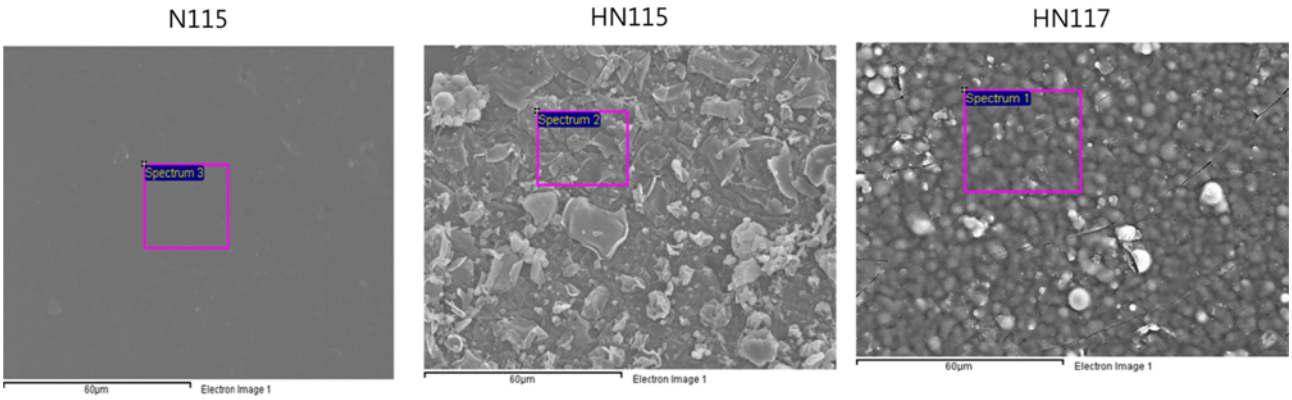

Element	Weight%	Atomic%
O K	0.00	0.00
F K	8.78	98.47
Si K	0.00	0.00
S K	0.23	1.53
Totals	9.01	

Element	Weight%	Atomic%
O K	1.35	17.38
F K	5.65	61.27
Si K	1.50	10.98
S K	1.61	10.37
Totals	10.12	

Element	Weight%	Atomic%
O K	1.71	29.63
F K	2.52	36.85
Si K	1.83	18.15
S K	1.77	15.38
Totals	7.83	

Fig. 4. SEM images and EDX analysis of membranes.

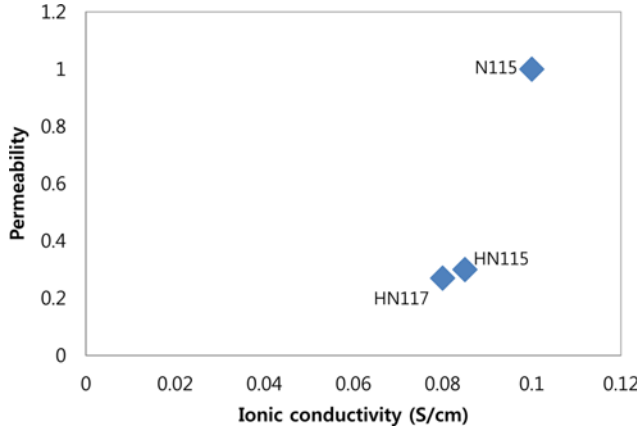

Fig. 5. Membrane selectivity in ionic conductivity and permeability.

ganic materials of SiO_2 were impregnated inside cluster of Nafion membrane, and then the sulfonation process performed the additional function of SiO_2 as proton conductors, as shown in Fig. 1. The inorganic proton conductor in polymer matrix exhibited higher ionic conductivity and lower permeability in HN115 and HN117.

2. Performance of VRFBs

The VRFB cells were tested at constant charging/discharging current density of 20 (2 cycles), 40 (3 cycles), 80 (3 cycles), 20 (3 cycles), 40 (3 cycles), 80 (3 cycles), and 20 (3 cycles) $mA{\cdot}cm^{-2}$. Fig. 6 illustrates the energy efficiency of VRFB cells with N115, HN115, and HN117. The energy efficiencies were obtained by using following equation:

$$EE\ (\%) = \frac{\int_0^t V_d I_d dt}{\int_0^t V_c I_c dt} \times 100\%,$$

where EE is the energy efficiency, V_d is the discharge voltage, I_d is the discharge current, V_c is the charge voltage, and I_c is the charge current.

The VRFB cell with N115 exhibited energy efficiencies of 70%, 72%, and 67% at 20, 40, and 80 $mA{\cdot}cm^{-2}$, respectively; the highest energy efficiency of 72% was achieved at 40 $mA{\cdot}cm^{-2}$. The energy efficiency of VRFB cells with hybrid membranes (HN115 and HN117) decreased with increases in the current density. The cell with HN115 exhibited energy efficiencies of 82%, 75%, and 64% at current densities of 20, 40, and 80 $mA{\cdot}cm^{-2}$, respectively. The cell with HN117 exhibited energy efficiencies of 70%, 63%, and 52% at current densities of 20, 40, 80 $mA{\cdot}cm^{-2}$, respectively. At the lowest current range of 20 $mA{\cdot}cm^{-2}$, the cell with HN115 exhibited the highest energy efficiency of 82%. However, at the highest current range of 80 $mA{\cdot}cm^{-2}$, the cell with N115 exhibited the highest energy efficiency value of 67%, which was higher than that of HN115. At the low current density of 20 $mA{\cdot}cm^{-2}$, the cell with HN115, which had 0.085 $S{\cdot}cm^{-1}$ of conductivity and 0.3 of permeability, exhibited the highest performances in energy efficiency. However, at the high current density of 80 $mA{\cdot}cm^{-2}$, N115, which had 0.1 $S{\cdot}cm^{-1}$ of conductivity (which was the highest conductiv-

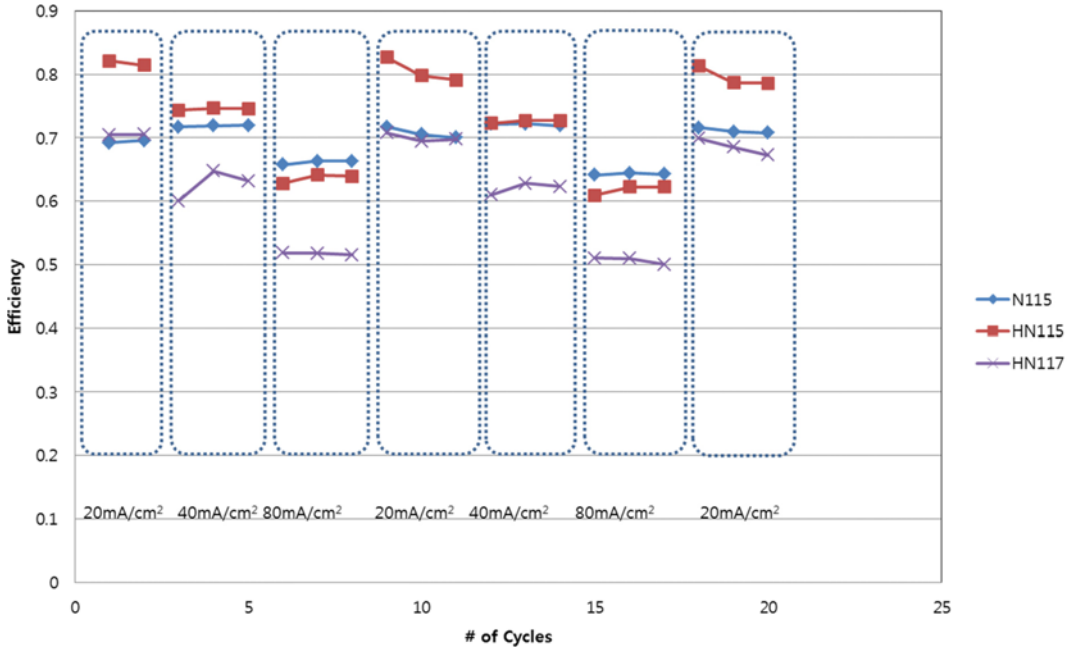

Fig. 6. Energy efficiencies of VRFB cells with membranes.

ity among the three membranes) and 1.0 of permeability, exhibited the highest performance. In the cells with HN115 and HN117 with increasing current densities, the membrane resistance approached ionic conduction, which increases the resistance and decreases the energy efficiency performances. For N115, the compromising effects of the ionic conductivity and permeability resulted in the maximum performance for the energy efficiency at a current density of 40 mA·cm^{-2}.

VRFB are technically similar both to a fuel cell and a battery. In low current ranges, the activation polarization is dominated by the redox activities of vanadium ions in the electrodes. In mid-current ranges, the internal polarization is dominated by the resistance of the membrane [31]. The transport losses are dominated in the solid electrode diffusion layers and liquid electrolyte due to a significant reduction of the vanadium ion concentrations in high current ranges. In the low current range of 20 mA·cm^{-2}, the redox activities of vanadium ions with composition of electrolyte should be dominant in the activation polarization, which is affected by permeability. The vanadium ions crossover resulted in the loss of appropriate ions in the electrolytes for VRFBs, which may affect the energy efficiencies. VRFBs with HN115 (low vanadium ion permeability) exhibit higher energy efficiency of 82% than those with N115 (high permeability). However, in the high current range of 80 mA·cm^{-2}, the ion transports through the membrane should be dominant for redox reaction of vanadium ions and correlated with the diffusion in the electrode layers and electrolyte, and the VRFB with N115 (higher ionic conductive membrane) shows the higher energy efficiencies than that with HN115. To obtain higher energy efficiencies, it is proposed that the ionic conductivity of the membranes contributes in the high current density range, and the permeability contributes in the low current density range. HN117 with the lower conductance of thicker membrane shows the comparable energy efficiency with N115 at the low current density range due to the lower permeability contribution. However, HN117 shows the lower energy efficiency than N115 at the high current density range, which results from the lower conductance of thicker membrane and the rough surface of HN117.

The columbic efficiency is the ratio between the energy removed from a battery during discharge compared with the energy used during charging to restore the original capacity. This is calculated as follows:

$$\mathrm{CE}\ (\%) = \frac{\int_0^t I_d dt}{\int_0^t I_c dt} \times 100\%,$$

where CE is the energy efficiency, I_d is the discharge current, and I_c is the charge current. The columbic efficiencies of the VRFB cells are presented in Fig. 7. The columbic efficiency of the cell with N115 exhibited 75%, 88%, 93% at 20 mA·cm^{-2}, 40 mA·cm^{-2}, 80 mA·cm^{-2}, respectively. The VRFB with N115 exhibited fluctuated columbic efficiency with the current density. The columbic efficiency in the VRFB with N115 had the lowest values of 75% at 20 mA·cm^{-2}, and the columbic efficiency increased with increases in the current density as seen in Fig. 7. However, the columbic efficiency of the VRFB cells with HN115 and HN117 was higher than 90% over the entire current density range; they exhibited similar values over the entire current range, which might result from the lower permeability of the vanadium ions than that in N115. Decreased columbic efficiency was observed in the higher permeable membrane of N115. The lower permeable membranes exhibited stable and higher columbic efficiencies over the entire current range in the VRFBs. This demonstrates that the columbic efficiency of VRFBs depends on the permeability of the vanadium ions through the membrane.

Fig. 8 plots the capacity and efficiency performances against the current density. As seen in Fig. 8(a), at a current density of 20 mA·cm^{-2}, the capacity of the VRFB cell with N115 during the charging

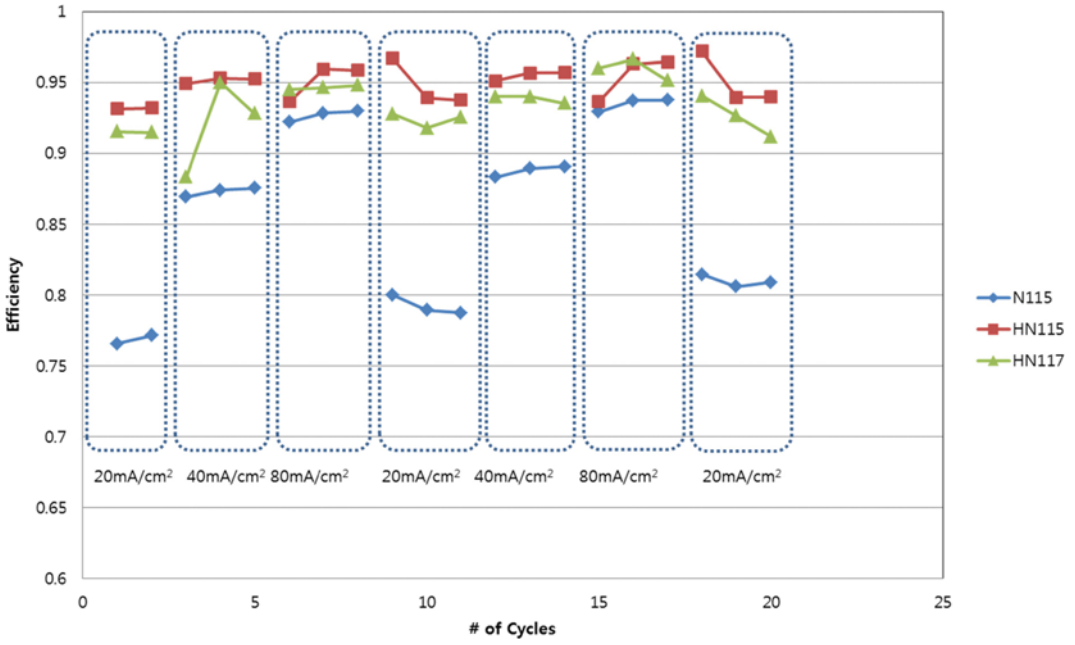

Fig. 7. Columbic efficiencies of VRFB cells with membranes.

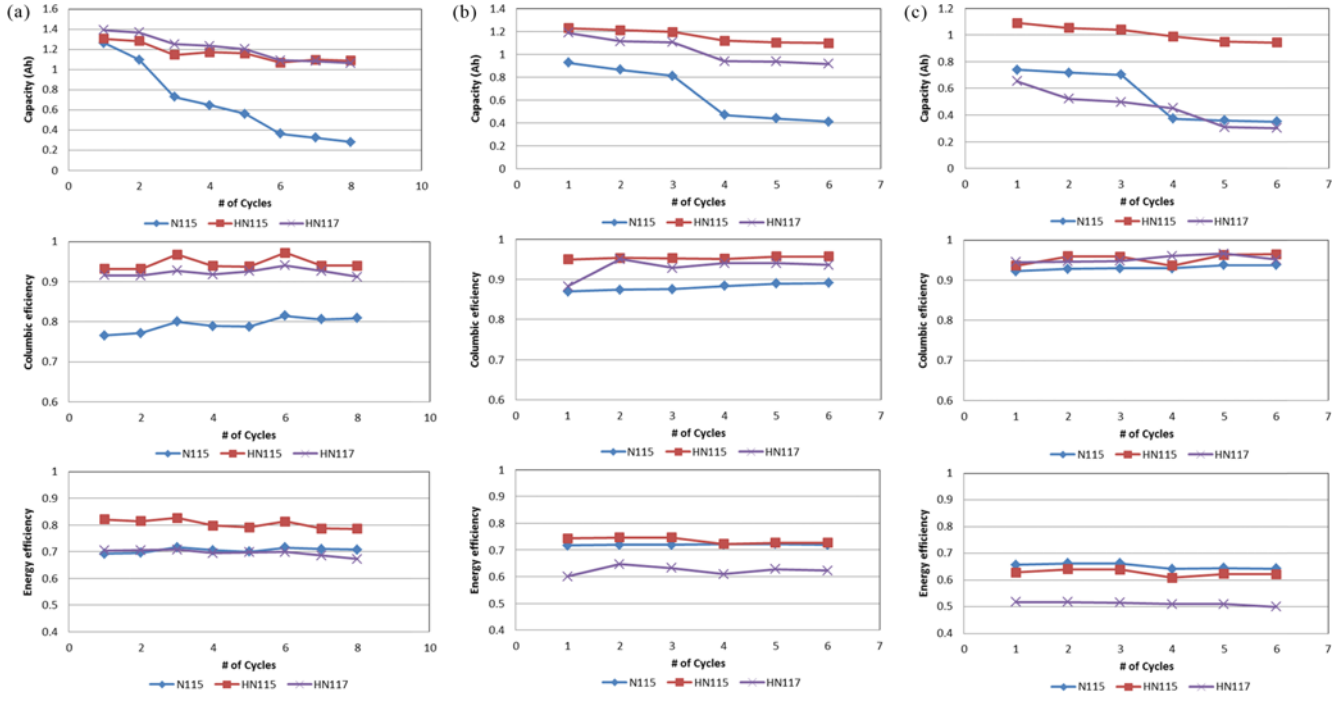

Fig. 8. Capacities, columbic efficiencies and energy efficiencies of (a) 20 mA·cm^{-2}, (b) 40 mA·cm^{-2} and (c) 80 mA·cm^{-2}.

decreased significantly from 1.25 Ah to 0.3 Ah. However, the cell with HN115 exhibited a capacity of 1.3 Ah and 1.1 Ah in the same conditions. The decreases in the charging capacities were more severe in N115 than HN115. With increases in the current density to 80 mA·cm^{-2}, the charging capacity of N115 decreased from 0.75 to 0.35 Ah. However, the cell with HN115 only decreased from 1.1 Ah to 0.95 Ah. HN117 exhibited a higher capacity at 20 mA·cm^{-2} and a lower capacities at 80 mA·cm^{-2}. The charging capacities in HN117 had gradual decrease with increase in the current density. The results demonstrate that the charging capacities are dependent on the permeability in low current density ranges and on the ionic conductivities in high current ranges. The VRFB performance demonstrated compromised effects of the membrane characteristics and operation conditions. Therefore, membrane development should be considered with the operation conditions and strategies when designing VRFBs.

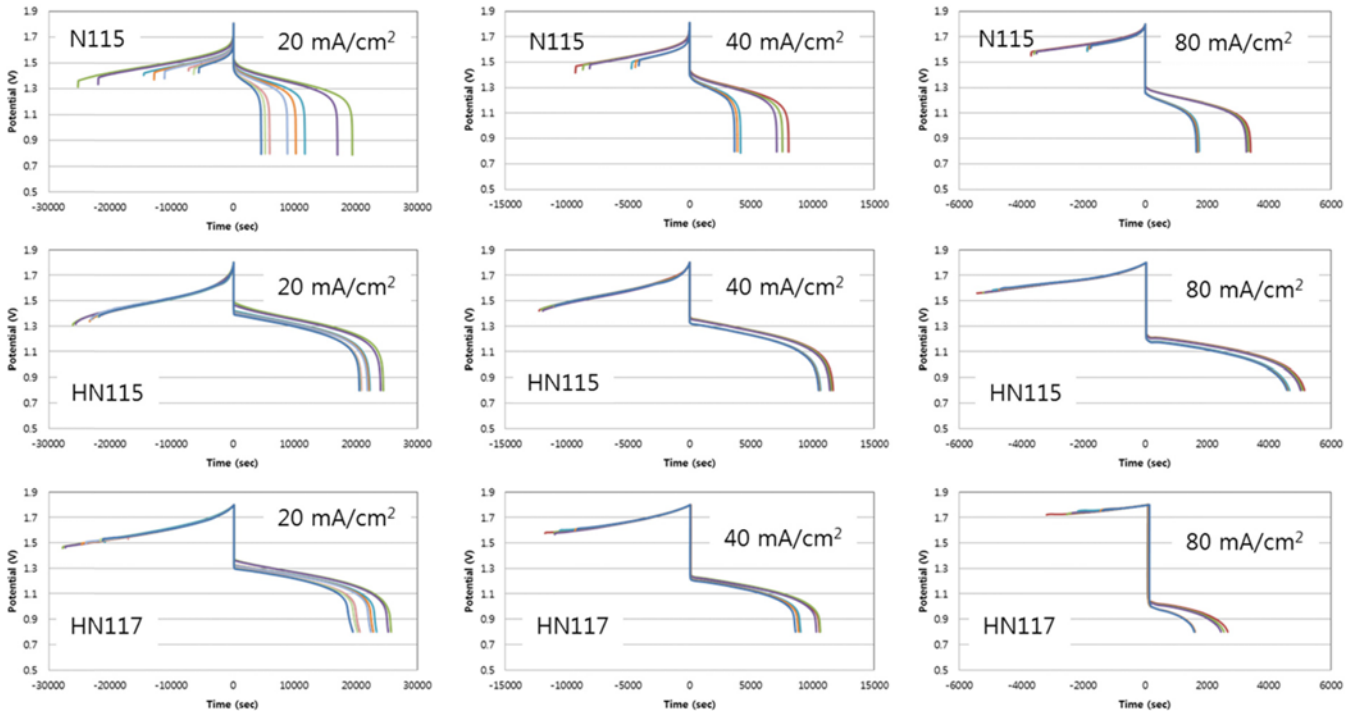

Fig. 9. Charging/discharging curves of RFB cells with membranes at various current densities.

The charging/discharging curves depict the improved performance of the hybrid membranes more clearly. As seen in Fig. 9, the discharging times shortened after repeating the charging/discharging tests. The time differences for discharging in N115 are easily observed in the charging and discharging curves. The lower depletion of the capacities in the VRFB with HN115 operated for longer times in the discharging cycles than in the VRFB with H115. During charging, at positive electrode, V^{+4} within the VO^{2+} ions was oxidized into V^{+5} within VO_2^+ ions; while at the negative electrode, V^{3+} were reduced to V^{2+}. The hydrogen ions $2H^+$ move through the membrane in order to maintain the electrical neutrality of the electrolytes. The standard open circuit voltage of a VRFB cell is E^o= 1.26 V at 25 °C; however, the real cells exhibited a higher E^o than 1.26 V due to the correcting Nernst's factors. During the charging/discharging measurements, the starting voltages for discharging were characterized, which is an instantaneous voltage drop for current loading. The ionic conductivity affected the discharging voltage, which caused the membrane with the higher ionic conductivity to exhibit fewer decreases in the voltage drop for discharging with increasing current density. With increasing current density, the instantaneous voltage decreased from 1.55 V to 1.32 V in N115, from 1.52 V to 1.25 V in HN115, from 1.39 V to 1.08 V in HN117, as seen in Fig. 10. It was observed that the voltage drop was dependent on the ionic conductivity of the membranes. Regarding the instantaneous voltage drop during the discharging, the VRFB cell with N115 exhibited the lowest voltage drop, and the VRFB cell with HN117 exhibited the highest voltage drop. The voltage drops for discharging result from the internal resistance and activation polarization. The higher ionic conductivity of the membrane and the catalytic activation of the electrolyte might contribute to the instantaneous voltage drop for discharging. The curves in Fig. 11

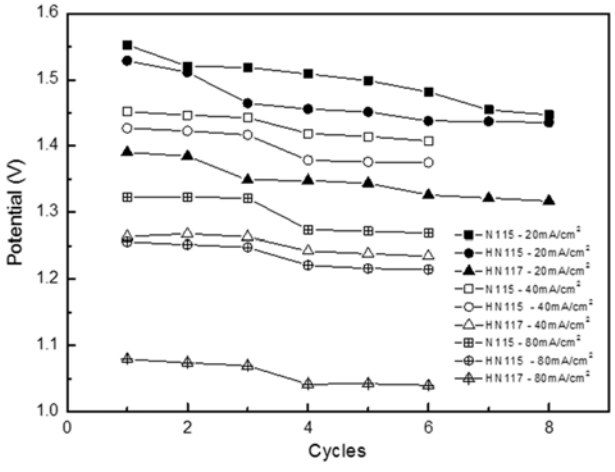

Fig. 10. Instantaneous voltage drops for discharging with membranes.

depict the polarization effects with the current density. The curves for discharging are very similar to fuel cell current-voltage curves. A wider discharging region was observed at a low current density of 20 mA·cm^{-2}. With increases in the current density, the ohmic region (i.e., capacity depletion time) narrowed. The VRFBs with the lower permeability of HN115 and HN117 exhibited broader ohmic regions, and the VRFB with the high ionic conductivity of N115 exhibited a lower voltage drop. In the VRFB with HN117, the voltage drop was the highest due to the lowest ionic conductivity; however, this VRFB exhibited the broadest discharging regions at 20 and 40 mA·cm^{-2}.

With the results of N115, HN115, and HN117, it is clear that the VRFB performance is dependent on the permeability and ionic

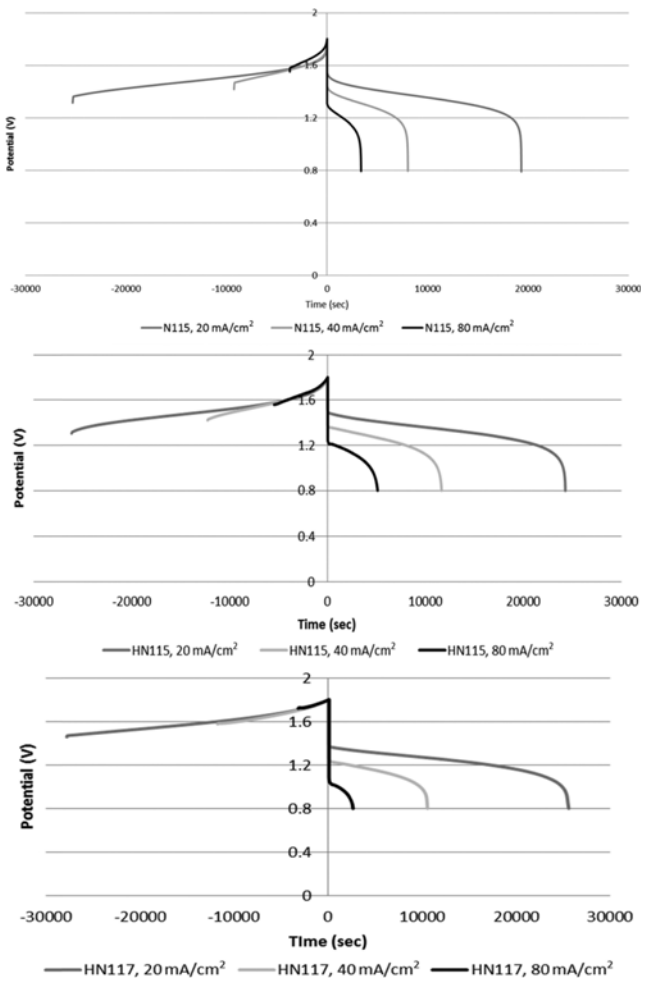

Fig. 11. Charging/discharging curves with current of RFB cells with various membranes.

conductivity of the membranes during operation conditions. The permeability properties are more dominant in low current density ranges, and the ionic conductivity is more effective in high current density ranges. The VRFB with lower permeable membranes exhibited higher energy efficiency and stable columbic efficiency. However, the lower ionic conductivity exhibited lower energy efficiency and higher voltage drops in the high discharging current range. To obtain higher performance, the membrane properties should be designed with consideration of the VRFB system operation.

CONCLUSIONS

Hybrid membranes were successfully fabricated through impregnation of inorganic proton conductors inside Nafion membranes. Hybrid membranes with Nafion115 (HN115) exhibited comparable ionic conductivity and 70% reduced permeability compared with Nafion115.

The VRFB cell with HN115 exhibited the highest energy efficiency of 82% at 20 $mA \cdot cm^{-2}$, and the VRFB cell with N115 exhibited the highest energy efficiency values of 67% at 80 $mA \cdot cm^{-2}$. In higher current range, the energy efficiencies with N115 had higher than HN115. The columbic efficiency with N115 exhibited lower values than those with HN115 and HN117, which resulted from the higher permeability of the vanadium ions than those of HN115 and HN117. From our results, the columbic efficiencies in VRFBs are more dependent on the membrane permeability and the energy efficiencies are dependent on the mixed performances of ionic conductivity and membrane permeability. The VRFB with lower permeable membranes (HN115) exhibited higher energy efficiency and stable columbic efficiency. Furthermore, the permeability of the membrane is a more dominant factor in low current density ranges and the ionic conductivity is more effective in high current density ranges.

The lower ionic conductive membrane (HN117) exhibited lower energy efficiency and higher voltage drops in the high discharging current range. The voltage drop was observed to depend on the ionic conductivity of the membranes. Regarding the instantaneous voltage for discharging, the VRFB cell with N115 exhibited the highest voltages and the VRFB cell with HN117 exhibited the lowest voltages at the tested current densities. The voltage drops for discharging resulted from the internal resistance and activation polarization. As a result, the development of membranes in VRFBs should be considered according to the operation conditions and membrane properties.

ACKNOWLEDGEMENT

This research was supported by Yeungnam University research grants in 2013.

REFERENCES

1. C. Menictas and M. Skyllas-Kazacos, *J. Appl. Electrochem.*, **41**, 1223 (2011).
2. C. Ponce de Leon, A. Frias-Ferrer, J. Gonzalez, D. A. Szanto and F. C. Walsh, *J. Power Sources*, **160**, 716 (2006).
3. Z. Yang, J. Zhang, M. C. W. Kintner-Meyer, X. Lu, D. Choi, J. P. Lemmon and J. Liu, *Chem. Rev.*, **111**, 3577 (2011).
4. N. Armaroli and V. Balzani, *Energy Environ. Sci.*, **4**, 3193 (2011).
5. G. Kear, A. A. Shah and F. C. Walsh, *Int. J. Energy Res.*, **36**, 1105 (2012).
6. A. Parasuraman, T. M. Lim, C. Menictas and M. Skyllas-Kazacos, *Electrochim. Acta*, **101**, 27 (2013).
7. X. Luo, Z. Lu, J. Xi, Z. Wu, W. Zhu, L. Chen and X. Qiu, *J. Phys. Chem. B*, **109**, 20310 (2005).
8. C. Yao, H. Zhang, T. Liu, X. Li and Z. Liu, *J. Power Sources*, **237**, 19 (2013).
9. N. Wang, S. Peng, Y. Li, H. Wang, S. Liu and Y. Liu, *J. Solid State Electrochem.*, **16**, 2169 (2012).
10. S. Kim, J. Yan, B. Schwenzer, J. Zhang, L. Li, J. Liu, Z. Yang and M. Hickner, *Electrochem. Commun.*, **12**, 1650 (2010).
11. S. Kim, T. B. Tighe, B. Schwenzer, J. Yan, J. Zhang, J. Liu, Z. Yang and M. A. Hickner, *J. Appl. Electrochem.*, **41**, 1201 (2011).
12. X. Ling, C. Jia, J. Liu and C. Yan, *J. Membr. Sci.*, **415-416**, 306 (2012).
13. D. Chen, S. Kim, L. Li, G. Yang and M. A. Hickner, *RSC Adv.*, **2**, 8087 (2012).
14. J. Pan, S. Wang, M. Xiao, M. Hickner and Y. Meng, *J. Membr. Sci.*,

443, 19 (2013).
15. N. Wang, J. Yu, Z. Zhou, D. Fang, S. Liu and Y. Liu, *J. Membr. Sci.*, **437**, 114 (2013).
16. C. Fujimoto, S. Kim, R. Stains, X. Wei, L. Li and Z. Yang, *Electrochem. Commun.*, **20**, 48 (2012).
17. M. J. Jung, J. Parrondo, C. G. Arges and V. Ramani, *J. Mater. Chem. A*, **1**, 10458 (2013).
18. S. Zhang, B. Zhang, D. Xing and X. Jian, *J. Mater. Chem. A*, **1**, 12246 (2013).
19. Z. Mai, H. Zhang, H. Zhang, W. Xu, W. Wei, H. Na and X. Li, *ChemSusChem*, **6**, 328 (2013).
20. D. Chen, M. A. Hickner, E. Agar and E. C. Kumbur, *Appl. Mater. Interfaces*, **5**, 7559 (2013).
21. J. Xi, Z. Wu, X. Teng, Y. Zhao, L. Chen and X. Qiu, *J. Mater. Chem.*, **18**, 1232 (2008).
22. X. Teng, Y. Zhao, J. Xi, Z. Wu, X. Qiu and L. Chen, *J. Membr. Sci.*, **341**, 149 (2009).
23. X. Teng, Y. Zhao, J. Xi, Z. Wu, X. Qiu and L. Chen, *J. Power Sources*, **189**, 1240 (2009).
24. Z. Mai, H. Zhang, X. Li, S. Xiao and H. Zhang, *J. Power Sources*, **196**, 5737 (2011).
25. N. Wang, S. Peng, D. Lu, S. Liu, Y. Liu and K. Huang, *J. Solid State Electrochem.*, **16**, 1577 (2012).
26. X. Teng, J. Dai, J. Su, Y. Zhu, H. Liu and Z. Song, *J. Power Sources*, **240**, 131 (2013).
27. X. Teng, C. Sun, J. Dai, H. Liu, J. Su and F. Li, *Electrochim. Acta*, **88**, 725 (2013).
28. Z. Li, J. Xi, H. Zhou, L. Liu, Z. Wu, X. Qiu and L. Chen, *J. Power Sources*, **237**, 132 (2013).
29. H. Kim and H. Chang, *J. Membr. Sci.*, **288**, 188 (2007).
30. L.Yang, B. Tang and P. Wu, *J. Membr. Sci.*, **467**, 236 (2014).
31. P. Alotto, M. Guarnieri and F. Moro, *Renw. Sust. Energy Rev.*, **29**, 325 (2014).